

Electronic supplementary information (ESI) for publication:

Phase equilibrium, dynamics and rheology of phospholipid-ethanol mixtures: A combined molecular dynamics, NMR and viscometry study

Fredrik Grote^a, Alexander Lyubartsev^a, Sergey V. Dvinskikh^b, Vibhu Rinwa^{a,c}, Jan Holmbäck^{a,c}

^a*Department of Materials and Environmental Chemistry, Stockholm University, Svante Arrhenius väg 16C, SE-106 91 Stockholm, Sweden*

^b*Department of Chemistry, KTH Royal Institute of Technology, 10044 Stockholm, Sweden*

^c*Lipidor AB, Svärdvägen 13, SE-182 33 Danderyd*

S1. Ethanol enthalpy of vaporization

In order to test how well the force field describes ethanol we computed enthalpy of vaporization according to $\Delta H_{\text{vap}} = H_{\text{gas}} - H_{\text{liquid}} = E_{\text{gas}} - E_{\text{liquid}} + RT$ where E_{liquid} is the average potential energy per molecule from a simulation of ethanol, E_{gas} is the potential energy of an isolated ethanol molecule, $R = 8.314 \text{ J}/(\text{mol K})$ is the gas constant and T is temperature. The obtained enthalpy of vaporization 39.4 kJ/mol is in good agreement with the value 38.82 kJ/mol reported from calorimetry experiments.¹ We found that the semi-empirical charges from the antechamber software gave better agreement with experimental enthalpy of vaporization than charges obtained by restrained electrostatic potential fitting.

S2. NMR spectra

Representative NMR spectra with assigned peaks are shown in Fig. S1. The labels refer to Fig. 1 of the main text.

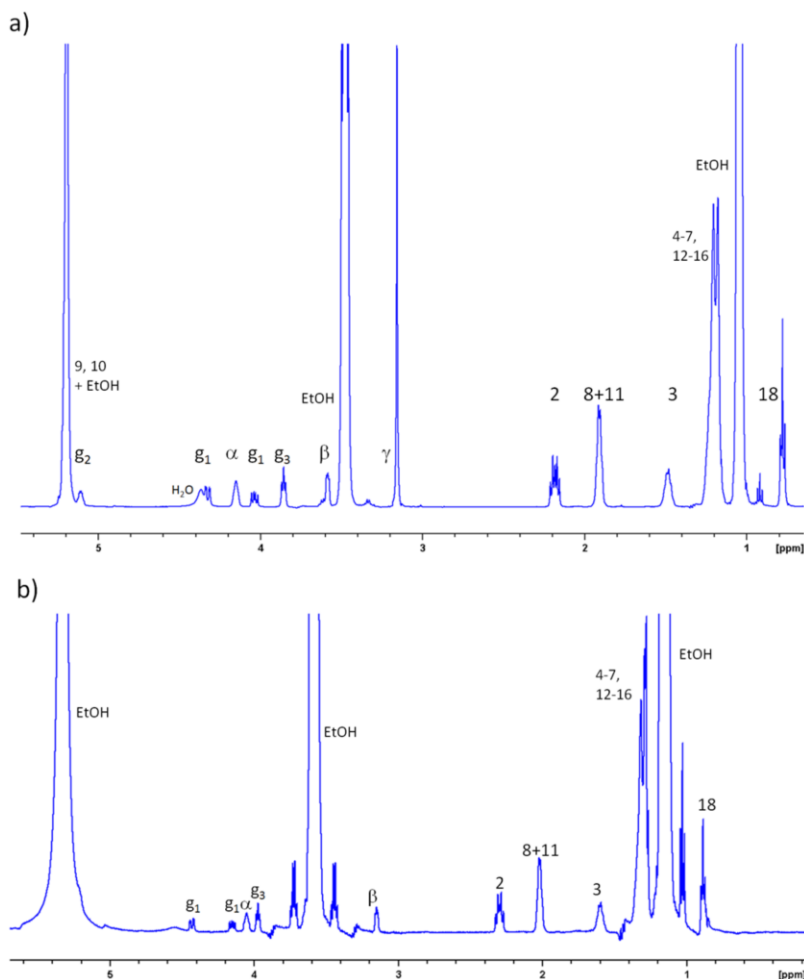


Fig. S1 ^1H NMR spectrum of (a) DOPC-ethanol mixture at concentration DOPC 29.81 wt% and (b) DOPE-ethanol mixture at concentration DOPE 4.97 wt%. For atom labelling, see the molecular structure in Figure 1 of the main text.

S3. Viscosity-shear rate plots

Viscosities were measured as function of shear rate, see Fig. S2. It was observed that viscosity is independent of shear rate and viscosities reported in Table 2 of the main text are averages of measurements at different shear rates and the uncertainties are the corresponding standard deviations.

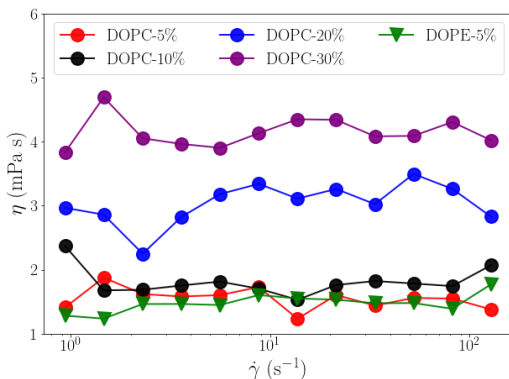


Fig. S2 Viscosity measured at different shear rates.

S4. Ethanol radial distribution functions

In order to better understand how the structure of ethanol around the lipid molecules change as function of lipid concentration we computed RDFs between atoms in lipids and ethanol molecules, see Fig. S3. The results indicate weak dependence on lipid concentration.

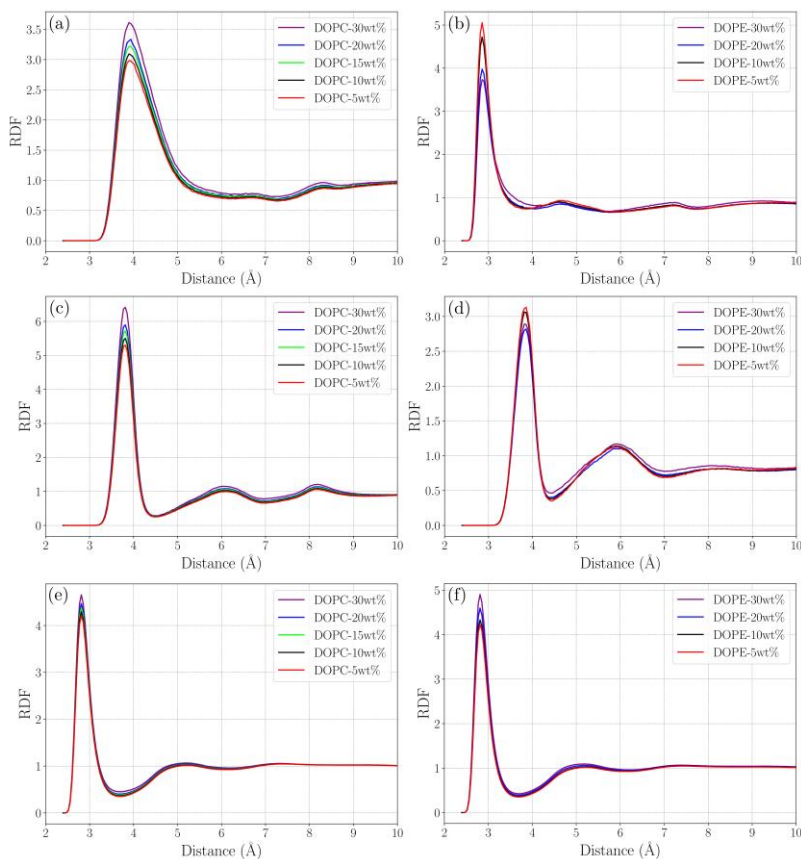


Fig. S3 Radial distribution functions calculated between (a) $N_{DOPC} - O_{EtOH}$, (b) $N_{DOPE} - O_{EtOH}$, (c) $P_{DOPC} - O_{EtOH}$, (d) $P_{DOPE} - O_{EtOH}$, (e) $O_{EtOH} - O_{EtOH}$ in system with DOPC and (f) $O_{EtOH} - O_{EtOH}$ in system with DOPE.

S5. RDF time window analysis

Since DOPE lipids showed strongest aggregation tendency we carried out an RDF time window analysis where we calculated the RDF between COM of DOPE lipids in different 50 ns time windows along the trajectory. This was done in order to investigate if the structure of the lipid-ethanol mixture was changing as function of time. The result shown in Fig. S4 indicates that the structure initially changes but becomes stable already after the first 100-200 ns of simulation.

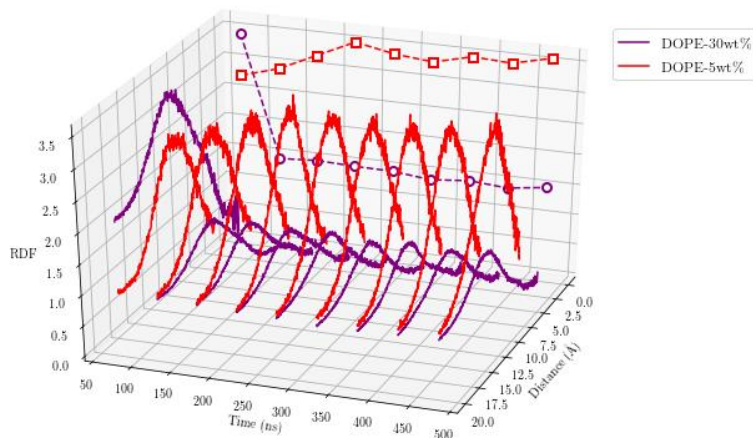


Fig. S4 RDFs between COM of DOPE lipids computed during different 50 ns time windows in the trajectory with the RDF maximum in each window projected onto the yz-plane.

S6. Mean square displacement

Diffusion coefficients for lipids and ethanol reported in Table 2 of the main text were computed from the slope of the MSD as function of lag time shown in Fig. S5-S6 together with logarithmic plots showing that the slope is close to 1.

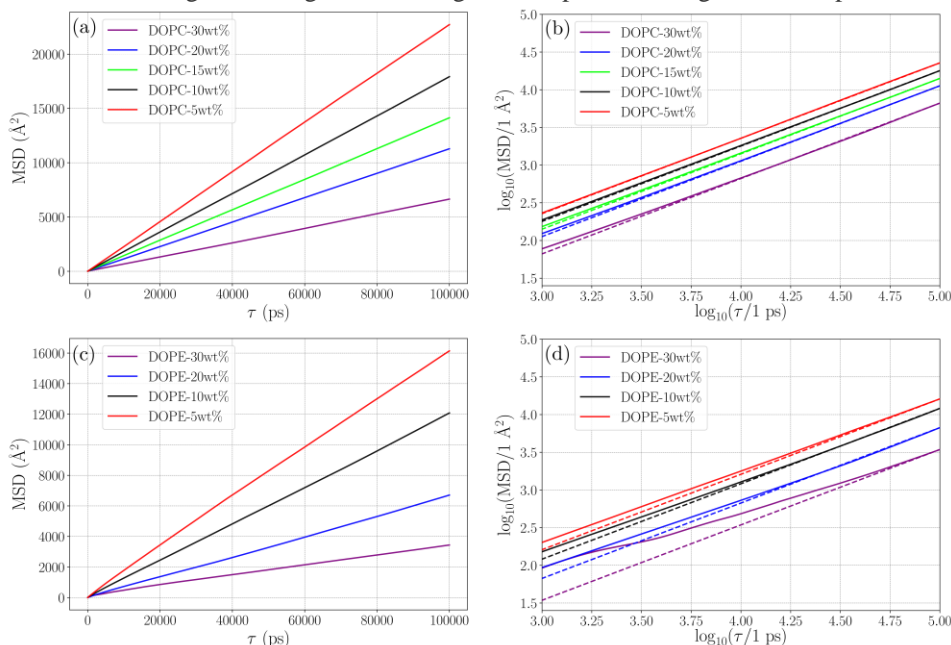


Fig. S5 Mean square displacement of lipid center of mass as function of lag time plotted on linear and logarithmic scale for (a)-(b) DOPC and (c)-(d) DOPE. In the logarithmic plots lines with slope equal to one that are tangent to the logarithm of MSD curves at long lag time are plotted to help show deviations from linearity (see dashed lines).

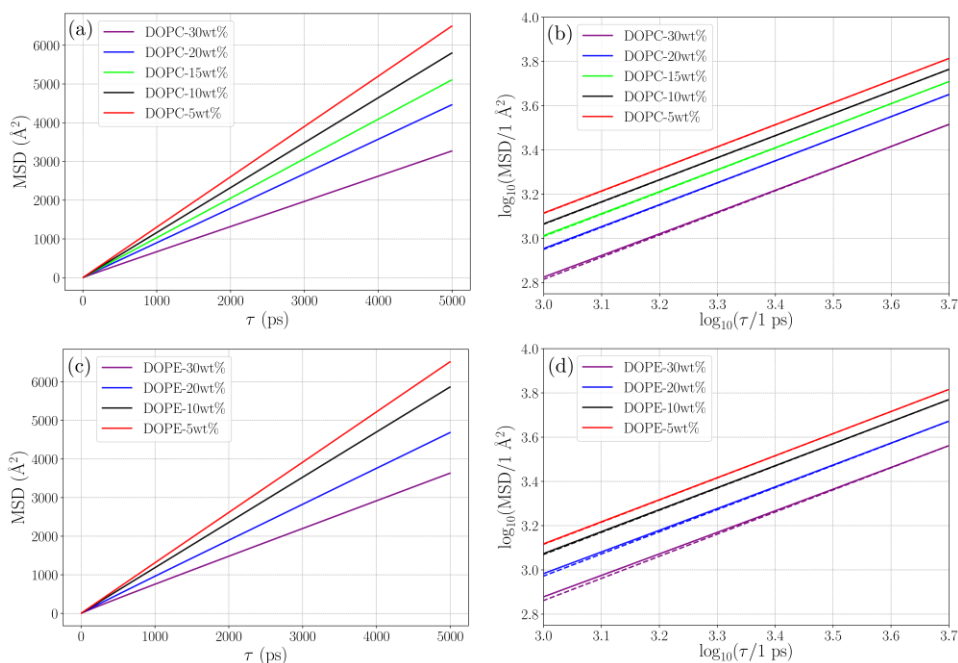


Fig. S6 Mean square displacement of ethanol center of mass as function of lag time plotted on linear and logarithmic scale for (a)-(b) DOPC and (c)-(d) DOPE. In the logarithmic plots lines with slope equal to one that are tangent to the logarithm of MSD curves at long lag time are plotted to help show deviations from linearity (see dashed lines).

S7. Correction of diffusion coefficients for periodic boundary conditions

Periodic boundary conditions can give artefacts when calculating diffusion coefficient from MD simulations. Yeh and Hummer² have suggested the following relation for correcting diffusion coefficients calculated from MD simulation of a periodic system with finite size:

$$D_{\infty} = D_L + k_B T \zeta / 6 \pi \eta L$$

where D_{∞} is the diffusion coefficient in an infinite system, D_L is the diffusion coefficient computed for a system under periodic boundary conditions with box length L , k_B is Boltzmann's constant, T is temperature, η is viscosity and $\zeta = 2.837298$ is a unitless constant. Diffusion coefficients corrected using eq. 1 are presented in Table S1.

Table S1 Diffusion coefficients for lipids and ethanol corrected for finite size effects using eq. 1.

System	$D_{\text{lipid},\infty}$ [$10^{-6} \times \text{cm}^2/\text{s}$]	$D_{\text{EtOH},\infty}$ [$10^{-6} \times \text{cm}^2/\text{s}$]
DOPC-5wt%	4.53	22.42
DOPC-10wt%	3.82	20.05
DOPC-15wt%	3.24	17.85
DOPC-20wt%	2.61	15.52
DOPC-30wt%	1.73	11.49
DOPE-5wt%	3.39	22.50
DOPE-10wt%	2.87	20.32
DOPE-20wt%	1.87	16.32
DOPE-30wt%	1.05	12.49

S8. NMR relaxation

Longitudinal relaxation times from NMR experiments are shown in Table S2.

Table S2 Longitudinal relaxation times T_1 (s) for protons in lipid molecules from NMR.

System	α	g1	g3	γ	2	8+11	3	18	EtOH CH ₂
DOPC-5wt%	0.49	0.43	0.43	0.47	0.61	0.85	0.52	1.81	2.86
DOPC-10wt%	-	-	-	-	0.68	0.94	0.62	2.03	2.85
DOPC-15wt%	0.51	0.47	0.46	0.44	0.64	0.80	0.63	1.96	2.62
DOPC-20wt%	0.50	0.48	0.47	0.43	0.64	0.78	0.64	1.83	2.55
DOPC-30wt%	0.47	0.47	0.45	0.38	0.61	0.71	0.58	1.72	2.32

We computed TCFs of the second order Legendre polynomial for different C-H bonds in lipid and ethanol molecules. For some C-H bond (C₁₈-H and C-H in the methylene group of ethanol) the TCF decayed to zero within 1 ns making it possible to integrate the TCF and calculate longitudinal relaxation times (T_1) using eq. 4 in the main text. Table S3 shows the obtained relaxation times.

Table S3 Longitudinal relaxation times T_1 (s) for protons in lipid molecules from MD.

System	18	EtOH CH ₂
DOPC-5wt%	6.81	34.94
DOPC-10wt%	6.39	31.57
DOPC-15wt%	6.41	30.62
DOPC-20wt%	6.52	28.31
DOPC-30wt%	5.83	24.62

S9 Convergence of Green-Kubo integral

Convergence of η (5 in the main text). Viscosity was calculated by numerical integration of the pressure tensor TCF (see eq. 15 in the main text). The convergence of η was checked by plotting the value of viscosity η as a function of the upper integration limit τ_{\max} , the Green-Kubo integral with respect to the upper integration limit η_{yz} as well as their average (η) as a function of τ_{\max} . In order to have good statistics in the TCF the longest time lag must be significantly shorter than the length of the time series from which the TCF was computed. We calculated the TCF from a 20 ns time series and our results are shown in Fig. S7. The plots indicate that the Green-Kubo integral converges already for $\tau_{\max} < 100$ ps.

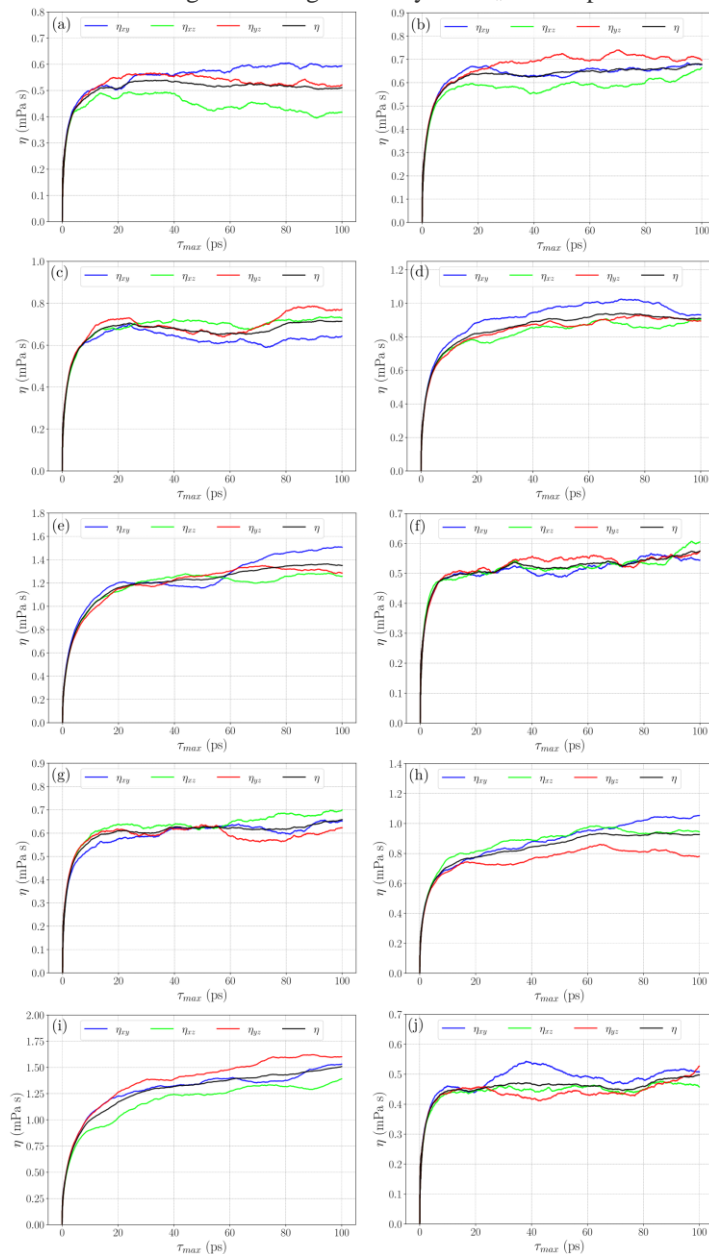


Fig. S7 Viscosity as function of upper integration limit in the Green-Kubo integral (τ_{\max}) computed from pressure-time series for systems: (a) DOPC-5wt%, (b) DOPC-10wt%, (c) DOPC-15wt%, (d) DOPC-20wt%, (e) DOPC-30wt%, (f) DOPE-5wt%, (g) DOPE-10wt%, (h) DOPE-20wt%, (i) DOPE-30wt%, (j) EtOH.

S10. Hydrodynamic radii

For the plots of diffusion coefficients, D , as function of reciprocal viscosity, η^{-1} , (see Fig. 8 in the main text) straight lines were fitted. Table S4 below shows the parameters (slope and intercept) for the fitted lines. The slope is related to the hydrodynamic radius R of diffusing lipids/lipid aggregates according to the Stoke-Einstein equation:

$$D = \frac{k_B T}{6\pi R} \times \eta^{-1}$$

where D is the diffusion coefficient, $k_B = 1.381 \times 10^{-23}$ J/K is Boltzmann's constant, T is temperature, R is hydrodynamic radius and η is viscosity.

Table S4 Slopes and intercepts for lines fitted to the plot of D versus η^{-1} (see Figure 8 in main text) and hydrodynamic radii (R) obtained from the Stoke-Einstein equation.

Data set	Slope ($10^{-13} \times \text{N}$)	Intercept ($10^{-6} \times \text{cm}^2/\text{s}$)	R (nm)
DOPC-MD	2.266	-0.684	1.0
DOPE-MD	1.798	-0.834	1.2
DOPC-Exp	3.754	0.166	0.6

References

- 1 D. M. T. Newsham and E. J. Mendez-Lecanda, Isobaric enthalpies of vaporization of water, methanol, ethanol, propan-2-ol, and their mixtures, *J. Chem. Thermodyn.*, 1982, **14**, 291-301.
- 2 I.C. Yeh and G. Hummer, System-size dependence of diffusion coefficients and viscosities from molecular dynamics simulations with periodic boundary conditions, *J. Phys. Chem. B*, 2004, **108**, 15873-15879.